Journal of Engineering Physics and Thermophysics, Vol. 81, No. 4, 2008

ON VIBRATION-CONVECTIVE FLOWS IN A HELE–SHAW CELL

I. A. Babushkin and V. A. Demin

UDC 532.516, 536.2:532/533

The influence of high-frequency horizontal vibrations on convective flow conditions in a Hele–Shaw cell located in a homogeneous gravitational field and heated from below has been studied theoretically and experimentally. The linear problem of stability of mechanical quasi-equilibrium in the case of model boundary conditions has been solved analytically. The supercritical conditions of vibrational convection have been investigated numerically by the finite-difference method. It has been shown that at small values of the thermal and vibration Rayleigh numbers in a fluid a state close to quasi-equilibrium is realized. The critical values of the thermal and vibration Rayleigh numbers at which a change of different stationary and nonstationary convective regimes takes place have been determined. A stability map of vibration-convective flows has been generated.

Introduction. The problem of investigating three-dimensional convective flow conditions has been the subject of many theoretical and experimental works. Using certain assumptions on the problem geometry, one can sometimes simplify the initial problem by reducing it to a two-dimensional one. Experience shows that even in the region of large supercriticalities often there is good agreement between experimental data and results of calculations obtained on the basis of two-dimensional models. A convective cavity that permits reducing a three-dimensional problem to a plane one is a Hele–Shaw cell. The free thermal convection of a homogeneous fluid in a below-heated Hele–Shaw cell with perfect heat-conducting wide faces and dimensions $1 \times 5 \times 10$ has been studied theoretically in [1]. As a result, it has been established that the first critical motion is the single-vortex motion in the plane of the wide faces of the cell. When stability is lost, this motion is replaced by the unstable four-vortex regime with a reconnection of the vortices.

In [2], the finite-difference method has been used to study numerically convective motions in a Hele–Shaw cell in zero gravity under the action of longitudinal high-frequency vibrations for various side ratios of the wide faces. However, only the first critical motions have been calculated. It has been shown that vibrational convection in zero gravity is excited "softly." V. Demin et al. [3] have found the conditions for the existence of mechanical quasi-equilibrium of a homogeneous fluid in a Hele–Shaw cell subjected to an external high-frequency action. The plane with perfect heat-conducting wide faces was considered. The scenarios of passing from quasi-equilibrium to irregular vibrations have been studied. It has been shown that in the presence of a strong vibrational action the first critical motion can be a two-vortex flow. The influence of vertical vibrations on the convection in a Hele–Shaw cell in a static gravitational field has been studied numerically and analytically in [4]. Calculations of finite-amplitude flows have been performed in a wide range of control parameters. It has been found that vertical vibrations increase the stability threshold of quasi-equilibrium.

Various stable and transient pulsation regimes of free thermal convection in a Hele–Shaw cell have been studied experimentally and theoretically in [5, 6]. In [5], we described stable single-vortex pulsation conditions where against the background of the main vortex in the corner of the cavity a small recurring vortex arises randomly, which in the course of time grows to certain sizes and is lost to the main stream. Then in the corner of the cavity a recurring vortex arises again and the process is repeated. In [6], we have investigated the specific transient regime representing a four-vortex flow symmetric about the vertical axis in the form of periodic pulsations of the lower convective cells with their partial absorption by the upper vortices.

The investigations of vibration-convective flows [3, 4] have been carried out in the approximation of a small thickness of the cavity when its wide faces are so large that the influence of the lateral faces can be neglected. Actually the equations of vibration convection do not admit a solution in the form of quasi-equilibrium for a Hele–Shaw

Perm State University, 15 Bukirev Str., Perm, 614990, Russia; email: demin@psu.ru. Translated from Inzhenerno-Fizicheskii Zhurnal, Vol. 81, No. 4, pp. 712–720, July–August, 2008. Original article submitted February 21, 2007.

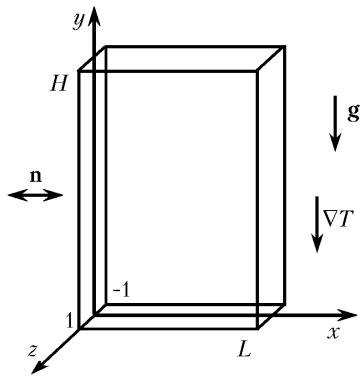

Fig. 1. Geometry of the problem and coordinate system.

cell with solid lateral boundaries. The condition of no flow onto the pulsation velocity component on the narrow faces leads to the fact that in the fluid a certain averaged flow should act as the ground state. The aim of the present work is to study theoretically and experimentally the influence of the narrow lateral faces on the vibrational convection of a homogeneous fluid in a Hele–Shaw cell heated below.

Formulation of the Problem. A Hele–Shaw cell is a cavity in the form of a rectangular parallelepiped, one of whose linear horizontal sizes is much smaller than the other two (Fig. 1). Let us choose as the unit of length the half-thickness of the cell; then H is the height of the cell and L is its length. In the experiment, the upper and lower faces were heat-exchangers, and the vertical faces were made of acrylic plastic. Therefore, in the calculations we shall assume that the horizontal faces are perfect heat-conducting and the vertical ones are heat-insulated. The cell is in a homogeneous gravitational field and is subjected to high-frequency horizontal vibrations oriented along the wide faces of the cavity. The temperature gradient maintained by the heat-exchanger on the vertical faces is directed downward, which corresponds to the heating from below.

Basic Equations. In the presence of high-frequency vibrations the flows in the reference system connected with the cavity are described by convection equations in the Boussinesq approximation by adding vibrational accelerations to the static acceleration of gravity. After the averaging and dedimensionalization procedure the system of equations of thermovibrational convection will have the following form [7]:

$$\frac{\partial \mathbf{v}}{\partial t} + \frac{1}{\mathrm{Pr}} (\mathbf{v}\nabla)\, \mathbf{v} = -\nabla p + \Delta \mathbf{v} + \mathrm{Ra}\, T\boldsymbol{\gamma} + \mathrm{Ra}_{\mathrm{v}}\, (\mathbf{w}\nabla)\, (T\mathbf{n} - \mathbf{w})\,, \tag{1}$$

$$\mathrm{Pr}\, \frac{\partial T}{\partial t} + (\mathbf{v}\nabla)\, T = \Delta T\,, \quad \mathrm{div}\, (\mathbf{v}) = 0\,, \tag{2}$$

$$\mathrm{rot}\, \mathbf{w} = \nabla T \times \mathbf{n}\,, \quad \mathrm{div}\, \mathbf{w} = 0\,. \tag{3}$$

Here $\mathbf{w}$ is the additional averaged vector field, which has the meaning of the amplitude of the pulsation velocity component and represents the solenoidal part of the field $T\mathbf{n}$.

We have chosen the following units of measurement of the physical quantities: $[d]$, half-thickness of the cell; $[d^2/\nu]$, time; $[\chi/d]$, velocity; $[\rho\nu\chi/d^2]$, pressure, and $[Ad]$, temperature.

System (1)–(3) contains dimensionless parameters: the Rayleigh number, the vibrational analog of the Rayleigh number, and the Prandtl number respectively:

$$\mathrm{Ra} = \frac{g\beta A d^4}{\nu\chi}\,, \quad \mathrm{Ra}_{\mathrm{v}} = \frac{(b\beta\Omega A d^2)^2}{2\nu\chi}\,, \quad \mathrm{Pr} = \frac{\nu}{\chi}\,.$$

The vibration amplitude b and the circular frequency Ω characterize the vibration effect on the hydrodynamic system.

The averaged velocity field on the solid faces satisfies the adhesion condition $\mathbf{v}\big|_{\mathrm{b}} = 0$. Because of the "non-viscous" character of high-frequency oscillations, the no-flow condition $w_{\mathrm{n}}\big|_{\mathrm{b}} = 0$ is placed on the amplitude of the pulsation velocity component. On the vertical faces the temperature gradient ∇T_0 corresponding to the heating from below is held constant.

Plane-Trajectory Approximation. The theoretical estimates and the experiments show that, even at large supercriticalities, motions of fluid particles in a Hele–Shaw cell lie in the plane of the wide faces. Thus, using the approximation L, $H >> d$, we assume the projections of the averaged and the pulsation velocity components on the z axis to be equal to zero $v_z = 0$, $w_z = 0$. This assumption makes it possible to introduce the stream functions: $\Psi(x, y, z)$ for the averaged velocity vector $\mathbf{v}(v_x, v_y, 0)$ and $\mathbf{\Phi}(x, y, z)$ for the amplitude of the pulsation velocity component $\mathbf{w}(w_x, w_y, 0)$

$$v_x = \frac{\partial \Psi}{\partial y}, \quad v_y = -\frac{\partial \Psi}{\partial x}; \quad w_x = \frac{\partial \Phi}{\partial y}, \quad w_y = -\frac{\partial \Phi}{\partial x}. \tag{4}$$

Substituting these expressions into (1)–(3), we obtain a system of equations in terms of the stream functions

$$\frac{\partial \varphi}{\partial t} + \frac{1}{\mathrm{Pr}}\left(\Psi_y \varphi_x - \Psi_x \varphi_y\right) = \Delta\varphi - \mathrm{Ra}\,\Theta_x + \mathrm{Ra_v}\left[\Phi_{yy}\Theta_x - \Theta_x + \Phi_{xy}\,(1 - \Theta_y)\right]; \tag{5}$$

$$\mathrm{Pr}\,\frac{\partial \Theta}{\partial t} + \left(\Psi_y \Theta_x - \Psi_x \Theta_y\right) + \Psi_x = \Delta\Theta; \tag{6}$$

$$\Delta_1 \Phi = \Theta_y, \quad \Delta_1 = \frac{\partial^2}{\partial x^2} + \frac{\partial^2}{\partial y^2}. \tag{7}$$

In Eqs. (5)–(7) the subscript denotes differentiation on the corresponding coordinate; $\varphi = \Delta_1 \Psi$ is vorticity; Δ_1 is the plane Laplace operator; Ψ, Φ, Θ are deviations of the fields from the equilibrium averaged values

$$\Psi_0 = 0, \quad \Phi_0 = \frac{1}{2}\, y\,(H - y), \quad T_0 = -y.$$

This solution describes the mechanical equilibrium state according to which in the fluid there is no averaged flow, but there are velocity fluctuations.

Linear Stability Problem. Consider a linear problem of mechanical equilibrium stability in the sense of small perturbations for a cell with heat-insulated wide faces. It admits a solution in the form

$$\Psi = \sum_{n,m} \psi_{nm} \sin\left(\frac{n\pi}{L}x\right)\sin\left(\frac{m\pi}{H}y\right)\cos\left(\frac{\pi z}{2}\right), \quad \Theta = \sum_{n,m} \theta_{nm} \cos\left(\frac{n\pi}{L}x\right)\sin\left(\frac{m\pi}{H}y\right),$$
$$\Phi = \sum_{n,m} \varphi_{nm} \cos\left(\frac{n\pi}{L}x\right)\cos\left(\frac{m\pi}{H}y\right), \tag{8}$$

where $n = 0, 1, 2, \ldots$; $m = 1, 2, 3, \ldots$. The Poisson equation (7) imposes such an expansion for Φ that the bulk force in the Navier–Stokes equation characterizing the vibrational action is nontrivial. The basis functions satisfy the model boundary conditions

$$x = 0, L: \ \Psi = \Psi_y = \Phi_x = \Theta_x = 0, \quad y = 0, H: \ \Psi = \Psi_x = \Phi_y = \Theta_x = 0,$$
$$z = \pm 1: \ \Psi_x = \Psi_y = \Theta_z = 0. \tag{9}$$

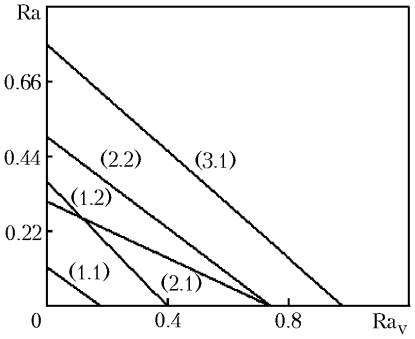

Fig. 2. Stability boundaries of mechanical quasi-equilibrium for various modes: *n*, first index; *m*, second index.

According to (9), the averaged velocity satisfies the conditions of no flow on the side walls and adhesion on the wide faces. The narrow vertical walls are heat-insulated, and on the upper and lower faces the temperature difference is held constant (the heat exchangers are isothermal).

After the linearization procedure we substitute solution (8) into the system of equations (5)–(7) and average over the cell width. In this case, expansions of (8) proceed through the equations, and a system of ordinary differential equations for the amplitudes ψ_{nm} and θ_{nm} is obtained. The Poisson equation for the stream function of the amplitude of the pulsation velocity component is not evolutional. It gives a system of algebraic equations which permits expressing the amplitudes of the stream function of the "pulsation" field φ_{nm} in terms of the corresponding amplitude coefficients θ_{nm} of the temperature field. Thus, the "vibrational force" in the Navier–Stokes equation is fully expressed in terms of the temperature field amplitude. The system of differential equations for ψ_{nm} and θ_{nm} has a solution in the form of normal disturbances, so that the stability boundary for monotone modes are obtained analytically:

$$\mathrm{Ra}_{nm} = \frac{\pi^6}{8}\left(1+\left(\frac{mL}{nH}\right)^2\right)\left[\left(\frac{n}{L}\right)^2+\left(\frac{m}{H}\right)^2+\frac{1}{4}\right]^2 - \mathrm{Ra}_V\left(1+\left(\frac{mL}{nH}\right)^2\right)^{-1}. \tag{10}$$

The critical Rayleigh values depend on the geometric parameters of the cell, the vibration Rayleigh number, and the form of the disturbance. Figure 2 graphically represents the results of the tabulation of formula (10) describing the stability boundary of mechanical quasi-equilibrium of the fluid for a cell of size $2 \times 20 \times 40$. It is seen that for a cell with heat-insulated wide faces the single-vortex disturbance characterized by mode (1, 1) is the most dangerous.

Nonlinear Problem. The linear stability problem was solved in the approximation of a small thickness of the cavity, which implied a negligibly weak influence of the lateral faces. However, formally the vibrational action can be arbitrarily strong and, as a result, in solving vibration convection equations one can no longer neglect the influence of the solid lateral faces. Let us show that the no-flow condition on the pulsation velocity component on the narrow faces leads to the fact that in the fluid a certain averaged flow acts as a ground state. Let us calculate the vibration convection in the Hele–Shaw cell with a complete set of boundary conditions by the grid method.

In the course of solving a complete (nonlinear) system of equations, the dependence of the stream function on the transverse coordinate z will, as before, be modeled by the trigonometric function

$$\Psi(x, y, z) = \psi(x, y)\cos\left(\frac{\pi z}{2}\right). \tag{11}$$

In order to satisfy the condition of heat insulation of the wide faces we assume that the temperature field is independent of the transverse coordinate. In this case, the requirement of heat insulation of the wide faces is satisfied automatically: $\partial\Theta/\partial z = 0$ at $z = \pm 1$. For the amplitude of the pulsation velocity component we have the no-flow condition; therefore, on the end faces

$$w_x(0) = w_x(L) = 0\,, \quad w_y(0) = w_y(H) = 0\,.$$

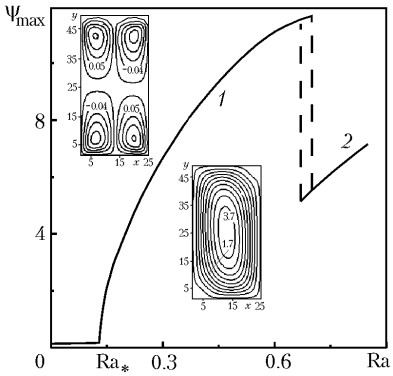

Fig. 3. Amplitude curves for small values of Ra_v: 1) single-vortex stationary flow; 2) two-vortex stationary flow.

In terms of the stream functions the boundary conditions take on the form

$$x = 0, L: \quad \psi = \frac{\partial \psi}{\partial x} = 0, \quad \Phi = 0, \quad \frac{\partial \Theta}{\partial x} = 0; \tag{12}$$

$$y = 0, H: \quad \psi = \frac{\partial \psi}{\partial y} = 0, \quad \Phi = 0, \quad \Theta = 0. \tag{13}$$

Upon averaging over the cell width the system of vibration convection equations together with the boundary conditions (12), (13) was solved numerically by the finite-difference method. In the course of the calculations, we used an explicit scheme in combination with the two-field technique [8]. In approximating the time derivatives and the coordinate derivatives, we used, respectively, one-sided differences and central differences. The Poisson equations for Φ and ψ were solved by the simple iteration method. In accordance with the experiment, calculations were performed for a cavity with a side ratio of 2 : 20 : 40. The number of nodes in the plane of the wide faces was equal to 27 × 49. The computer modulus was written in Fortran-90. In seeking solutions, the determination method was used.

Experimental. For the experimental studies, we made a cell of height 40 mm, length 20 mm, and thickness 2 mm. The cell was placed on the commutator-motor-controlled table of the shaker. The table with the cell executed reciprocating motions along the horizontal axis. The use of the commutator motor permitted smooth variation of the vibration frequency from 0 to 10 Hz in the course of the experiment. The vibration amplitude of the shaker carriage was 6 cm.

In visual observations and video photography, we used a special circuit for synchronous triggering of the flash bulb. In the experiments, we changed sequentially the temperature difference between the heat exchangers with fixed amplitude and vibration frequency of the shaker carriage or in the case of constant amplitude and temperature difference we varied the vibration frequency. For the working fluid, transformer oil was used in the experiments. To visualize convective flows, we added into the working fluid light-scattering aluminum powder particles. We could observe with their help both the motion pattern in general and the trajectories of individual particles. The presence of a small number of particles in the investigated fluid did not affect its physical properties. The structure of the flows was registered by means of a digital video camera. Video rolls were broken up into frames and computer-processed with the aid of an "Adobe Photoshop" graphics editor. Images in the frames were superimposed on one another, as a result of which the image obtained represented an analog of a long-exposure photograph in which tracks of moving particles are well defined.

Results and Discussion. If the influence of the narrow side walls is insignificant, then from the analysis of the linear stability problem it follows that at small values of the thermal and vibration Rayleigh numbers in the Hele–Shaw cell the state of mechanical quasi-equilibrium should exit. The numerical solution of nonlinear equations with correct boundary conditions on Φ corresponding to the no-flow condition for **w** shows that at small values of the vibration Rayleigh number in the fluid a flow with a very small amplitude is established. This stationary flow represents

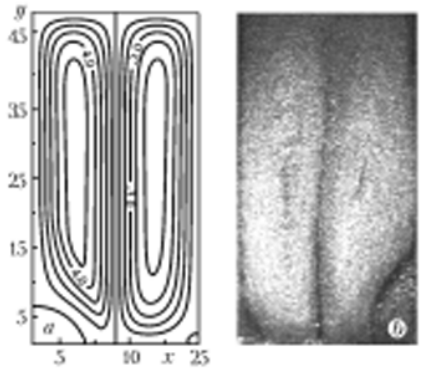

Fig. 4. Two-vortex flow: a) theory; b) experiment.

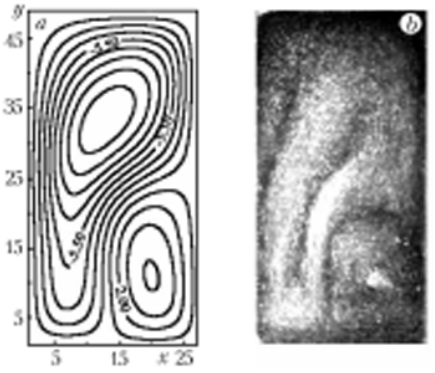

Fig. 5. Pulsation regime: a) theory; b) experiment.

four symmetric vortices whose intensity maxima are localized in the corners of the cavity, and in the center a dead zone is formed. With increasing Rayleigh number this regime loses stability and in the fluid there arises "softly" a single-vortex flow that occupies the whole of the cavity. Figure 3 shows the amplitude curve for $Ra_v = 0.1$ and Pr = 1.0 illustrating the transition to a single-vortex flow. It is seen that below Ra_* in the fluid a state close to quasi-equilibrium is in fact realized: the amplitude of the initial flow is incomparably small compared to the amplitude of the single-vortex regime.

Experiments confirm the existence of quasi-equilibrium for small values of the vibration Rayleigh number. Visual observations in the range of $Ra_v = 0–0.1$ show the absence of averaged flows in the fluid below the stability threshold of the single-vortex flow.

With a further increase in the Rayleigh number the single-vortex flow becomes unstable and is replaced by a two-vortex stationary flow. The results of the calculation of the stream function field are presented in Fig. 4a for Ra = 0.7 and $Ra_v = 0.1$. In the experiment, the passing to two-vortex flows takes 2 h. The vortex in one of the lower corners of the cavity increases monotonically in size, gradually displacing the main vortex into the other half. As the calculations show and the experiments confirm, the replacement of the single-vortex flow by the two-vortex one occurs with a hysteresis (Fig. 3). With increasing Rayleigh number the two-vortex convective flow remains stationary, and only the rotational velocity grows.

At Ra = 0.9 the two-vortex flow becomes unstable and, as a result of the Hopf bifurcation, vibrations in the form of corner vortex pulsations against the background of the asymmetric single-vortex flow are established (Fig. 5). The pulsation regime is established in the following way: the symmetry of the vortices breaks and one of them begins to grow, displacing the other one into the lower corner. At the same time in the opposite upper corner of the cavity a small additional vortex with a reverse flow is generated. Then the lower suppressed vortex begins to grow and at some instant of time upon reaching about one-third of the height is entrained by the main stream, after which again in the same lower corner of the cavity there appears a vortex which also grows and the process of coalescence with the main stream is repeated. Figure 5a shows the stream function field at Ra = 0.7 and $Ra_v = 0.1$, illustrating the pul-

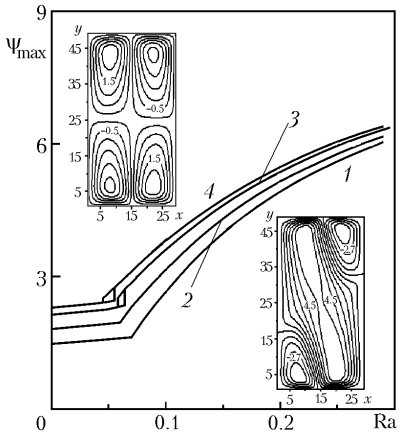

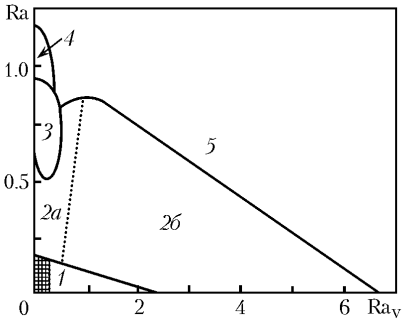

Fig. 6. Amplitude curves under the action of intensive vibrations: 1) Ra_V = 0.9; 2) 1.1; 3) 1.3; 4) 1.4.

Fig. 7. Stability map: 1a) state close to quasi-equilibrium; 1b) four-vortex thermovibration flow; 2a) single-vortex with soft excitation; 2b) single-vortex regime with secondary corner vortices; 3) two-vortex flow; 4) pulsation regime; 5) four-vortex nonstationary regime with a reconnection of vortices.

sation regime at a certain instant of time. The given pulsations of the lower cell near the asymmetric single-vortex flow are realized in the range of Rayleigh numbers Ra = 0.9–1.2 and represent a stable regime of fluid-induced vibrations. In the experiment, the process recurs at intervals of about 5 min depending on the temperature difference.

The quasi-equilibrium state is characteristic for small values of the vibration Rayleigh number. With increasing Ra_V the amplitude of the main four-vortex flow grows and becomes comparable to the amplitude of the secondary flow. The transition to a secondary flow occurs when two diagonal corner vortices coalesce to form one large vortex displacing the other two reverse-twist vortices (fragment in Fig. 6). In essence, this is a single-vortex flow predictable by the linear theory, whose form has been disturbed because of the interaction with the background thermovibrational flow arising due to the influence of the solid lateral faces. Figure 6 presents the family of amplitude curves for various values of the Rayleigh vibration number which illustrates the transition from the main four-vortex flow to a secondary flow. Comparing Figs. 3 and 6, it may be concluded that the symmetric single-vortex regime is gradually transformed to a three-vortex flow with one main and two secondary vortices with increasing Rayleigh vibration number. It is seen that there exists a range of Rayleigh vibration numbers at which the secondary stationary three-vortex flow arises "rigidly."

The stability boundaries of the vibration-convective regimes obtained by the results of numerical calculations are given in Fig. 7. The shaded region on the map of regimes corresponds to a state close to quasi-equilibrium. The existence of mechanical quasi-equilibrium in a Hele–Shaw cell has been tested experimentally. With increasing Rayleigh number this state is replaced by a regular single-vortex stationary flow (region 2a, Fig. 7). Region 2 is arbitrarily divided by a line into two parts. At larger Rayleigh vibration numbers a clearly defined stationary three-vortex flow with one main and two secondary flows in the corners of the cavity takes place (region 2b, Fig. 7). The design of the experimental facility did not enable us to attain larger values of the Rayleigh vibration number in the experiments and to observe this regime. Further, with increasing control parameters there arises a four-vortex vibration mode with a reconnection of vortices (region 5, Fig. 7), which at sufficiently large supercriticalities becomes stochastic. In the experiment the transition from pulsations to vibrations begins with the downward propagation of the upper corner vortex. Then its reconnection with the lower vortex in the opposite corner of the cavity occurs. The characteristic stages of this vibrational mode can be found in [1, 6]. If the values of the Rayleigh vibration number are sufficiently large, then the four-vortex regime with a reconnection of vortices arises as soon as the stationary three-vortex flow with two secondary vortices loses stability (passing from region 2b to 5).

Note that in the experiment in the absence of vibrations at Ra ≥ 2.1 a transient flow in the form of four vortices symmetric about the vertical axis sometimes arose. At a certain instant of time the lower vortices begin to grow, extending along the vertical axis of the cell to the cavity center with the upper flows pressing them to the symmetry axis on the side of the lateral walls. Then the upper part of the lower vortices is completely entrained by the convec-

tive cells above, and the vortices in the lower corners of the cell occupy a region of about $h/3$ again. Such pulsations occur 5–10 times with a periodicity of about 90 sec, after which the diagonal cells coalesce and a four-wave vibrational mode with a reconnection of vortices is established. This pulsation transient regime is described in detail in [6] on the basis of both theoretical and experimental studies. To realize this transient pulsation regime, we had to use in the calculations the initial conditions for the stream function and temperature fields symmetric about the vertical axis. When vibrations were "switched on," such a regime was not observed.

Comparison of the experimental data and the results of the calculations points to different boundaries for the corresponding regimes. In the calculations, the stability threshold of mechanical equilibrium, as well as the stability boundaries of the one-vortex, two-vortex, and pulsation flows, as well as of the four-vortex vibrational mode with a reconnection of vortices, are much lower than the experimental values. The experimental photograph of the two-vortex flow is shown in Fig. 4b for Ra = 1.66 and $\mathrm{Ra_v} = 0.029$ ($\nu = 2.82$ Hz). The form of the pulsation flow in Fig. 5b is given for Ra = 1.8 and $\mathrm{Ra_v} = 0.01$ ($\nu = 1.56$ Hz). This is explained by the fact that in the calculations we used the condition of heat insulation of the wide faces, whereas in the experimental model the wide faces are made of acrylic plastic, which corresponds to the intermediate heat conductivity of the boundaries. The theoretical studies made for perfect heat-conducting wide faces give an entirely different sequence of convective regimes. The present calculations made for heat-insulated wide faces adequately describe the form and sequence of convective regimes with changing control parameters of the problem and predict the specific flows in the range of large values of the Rayleigh vibration number.

Conclusions. Stable and transient vibration-convective flows in a below-heated Hele–Shaw cell have been investigated. A stability map of convective regimes has been compiled for a wide range of control parameters. It has been shown theoretically that at small values of the Rayleigh thermal and vibration numbers the averaged flow intensity is low and in the fluid a state close to quasi-equilibrium is realized. Experiments confirming the existence of mechanical quasi-equilibrium whose stability boundary is in good agreement with the analytical formula have been performed. In the region of large values of the vibration parameters, the ground state represents a four-vortex thermovibration flow. When stability is lost, the diagonal vortices reconnect and a stationary single-vortex flow with corner vortices arises. The vibration-convective regimes obtained in the numerical calculations in the range of small values of the vibration parameter agree with all the flows observed in the experiment.

We wish to thank D. V. Lyubimov and G. F. Putin for helpful discussions.

The work was supported by the Russian Foundation for Basic Research, projects Ural-2007 No. 07-08-96035 and No. 07-08-97620.

NOTATION

A, characteristic temperature gradient, K/m; b, vibration amplitude, m; d, half-thickness of the cavity, m; $\mathbf{g}$, gravitational vector, $\mathrm{m/sec^2}$; g, value of the gravitational acceleration, $\mathrm{m/sec^2}$; h, cavity height in the experiment, m; H and L, cavity height and length in the calculations; $\mathbf{n}$, unit vector directed along the vibration axis; n, m, mode numbers; $p(x, y)$, pressure field, $\mathrm{N/m^2}$; Pr, Prandtl number; Ra, Rayleigh number; $\mathrm{Ra_v}$, vibration analog of the Rayleigh number; t, time, sec; $T(x, y)$, temperature field, K; ∇T, temperature gradient at the cavity boundaries, K/m; $\mathbf{v}$, velocity field, m/sec; $\mathbf{w}$, amplitude of the pulsation velocity component, K; x, y, z, Cartesian coordinates; β, coefficient of thermal expansion, 1/K; $\boldsymbol{\gamma}$, unit vector directed vertically upward; θ, temperature field amplitude; Θ, deviation of the temperature from the equilibrium value, K; ν, kinematic viscosity coefficient, $\mathrm{cm^2/sec}$; ρ, fluid density, $\mathrm{kg/m^3}$; $\varphi(x, y)$, velocity field of the vortex, 1/sec; $\Phi(x, y)$, stream function for the amplitude of the pulsation velocity component, K·m; χ, thermal diffusivity, $\mathrm{cm^2/sec}$; ψ, amplitude of the stream function; $\Psi(x, y)$, stream function for the averaged velocity, $\mathrm{m^2/sec}$; Ω, cyclic vibration frequency, 1/sec. Subscripts: max, maximum; *, critical value; b, cavity boundaries; n, normal vector component; 0, equilibrium value; v, vibration.

REFERENCES

1. D. V. Lyubimov, G. F. Putin, and V. I. Chernatynskii, On convective motions in the Hele–Shaw cell, *Dokl. Akad. Nauk SSSR*, **235**, No. 3, 554–556 (1977).

2. L. M. Braverman, On vibrational thermal convection in the Hele–Shaw cell, in: *Convective Flows*, *Mezhvuz. Sbornik Nauch. Trudov*, Izd. Perm Ped. Inst., Perm' (1989), pp. 73–78.
3. V. A. Demin and I. S. Faizrakhmanova, Stability of vibrational- convective motions in the Hele–Shaw cell, *Vestn. Perm Univ.*, *Fizika*, Issue 1, 108–113 (2003).
4. V. A. Demin and D. V. Makarov, Stability of convective flows in the Hele–Shaw cell under the action of vertical vibrations, *Vestn. Perm Univ.*, *Fizika*, Issue 1, 101–110 (2005).
5. I. A. Babushkin and V. A. Demin, Experimental and theoretical investigation of transient convective regimes in the Hele–Shaw cell, *Izv. Ross. Akad. Nauk*, *Mekh. Zhidk. Gaza*, No. 3, 3–9 (2006).
6. I. A. Babushkin and V. A. Demin, Capture of convective vortices by a nonstationary flow in a Hele–Shaw cell, *Inzh.-Fiz. Zh.*, **80**, No. 1, 100–106 (2007).
7. G. Z. Gershuni, E. M. Zhukhovitskii, and A. A. Nepomnyashchii, *Stability of Convective Flows* [in Russian], Nauka, Moscow (1989).
8. E. L. Tarunin, *Computating Experiment in Free Convection Problems* [in Russian], Izd. Irkutsk Univ., Irkutsk (1990).